

Article

Synthesis and Fluorescence Properties of Structurally Characterized Heterobimetallic Cu(II)–Na(I) Bis(salamo)-Based Complex Bearing Square Planar, Square Pyramid and Triangular Prism Geometries of Metal Centers

Xiu-Yan Dong, Qing Zhao, Zhi-Li Wei, Hao-Ran Mu, Han Zhang and Wen-Kui Dong * 

School of Chemical and Biological Engineering, Lanzhou Jiaotong University, Lanzhou, Gansu 730070, China; dxy568@163.com (X.-Y.D.); zq18215194507@163.com (Q.Z.); wzl254452590@163.com (Z.-L.W.); muhaoran121@163.com (H.-R.M.); 13572510846@163.com (H.Z.)

* Correspondence: dongwk@126.com; Tel.: +86-931-493-8703

Received: 27 March 2018; Accepted: 23 April 2018; Published: 25 April 2018



Abstract: A novel heterotrinnuclear complex $[\text{Cu}_2(\text{L})\text{Na}(\mu\text{-NO}_3)]\cdot\text{CH}_3\text{OH}\cdot\text{CHCl}_3$ derived from a symmetric bis(salamo)-type tetraoxime H_4L having a naphthalenediol unit, was prepared and structurally characterized via means of elemental analyses, UV-Vis, FT-IR, fluorescent spectra and single-crystal X-ray diffraction. The heterobimetallic Cu(II)–Na(I) complex was acquired via the reaction of H_4L with 2 equivalents of $\text{Cu}(\text{NO}_3)_2\cdot 2\text{H}_2\text{O}$ and 1 equivalent of NaOAc. Clearly, the heterotrinnuclear Cu(II)–Na(I) complex has a 1:2:1 ligand-to-metal (Cu(II) and Na(I)) ratio. X-ray diffraction results exhibited the different geometric behaviors of the Na(I) and Cu(II) atoms in the heterotrinnuclear complex; the both Cu(II) atoms are sited in the N_2O_2 coordination environments of fully deprotonated $(\text{L})^{4-}$ unit. One Cu(II) atom (Cu1) is five-coordinated and possesses a geometry of slightly distorted square pyramid, while another Cu(II) atom (Cu2) is four-coordination possessing a square planar coordination geometry. Moreover, the Na(I) atom is in the O_6 cavity and adopts seven-coordination with a geometry of slightly distorted single triangular prism. In addition, there are abundant supramolecular interactions in the Cu(II)–Na(I) complex. The fluorescence spectra showed the Cu(II)–Na(I) complex possesses a significant fluorescent quenching and exhibited a hypsochromic-shift compared with the ligand H_4L .

Keywords: symmetric bis(salamo)-type tetraoxime; heterobimetallic complex; synthesis; crystal structure; spectroscopic study

1. Introduction

A wide variety of N_2O_2 -donor chelate ligands have been proverbially used to prepare alkaline earth, rare earth, and transition metal complexes for several decades. More recently, modified salen-type ligands having imine groups ($-\text{C}=\text{N}-$) [1–8], bear the potentially tetradentate N_2O_2 -donor and can form relatively stable complexes with different metal ions. Salen and its derivatives are extremely attractive and commonly versatile ligands because their metal complexes have been studied in potential application in catalyses [9,10], supramolecular architectures [11–19], luminescence properties [20–26], electrochemical conducts [27,28], biological systems [29–37], optical sensor [38,39], magnetic materials [40–45] and nonlinear optical materials [46], and so forth. A lot of researches have been fulfilled to design and synthesize mono-nuclear and homo- or hetero-polynuclear metal complexes possessing salen-type or salamo-type ligand or its analogues. Compared to salen,

salamo-type ligand [47–56] has a $-\text{CH}=\text{N}-\text{O}-(\text{CH})_n-\text{O}-\text{N}=\text{CH}-$ configuration and its corresponding complexes are more stable relatively.

The bis(salamo)-type ligand H_4L containing O_6 coordination sphere was already prepared earlier to obtain a series of $\text{Zn}(\text{II})-\text{M}(\text{II})$, $\text{Co}(\text{II})-\text{M}(\text{II})$ ($\text{M} = \text{Ca}, \text{Sr}$ and Ba) and $\text{Zn}(\text{II})-\text{RE}(\text{III})$ ($\text{RE} = \text{La}, \text{Ce}$ and Dy) complexes. Therefore, these compounds are considered to be heterotrimeric bis(salamo)-type complexes. Meanwhile, the crystal structures and properties of the obtained complexes have been studied in detail [28,57–59]. Owing to the bis(salamo)-type ligand H_4L bearing an O_6 coordination sphere, it can form homotrimeric bis(salamo)-type complexes. The transition metal atom located in O_6 coordination sphere can be replaced by alkali metal atoms with a larger atomic radius. To study the structural characteristics and fluorescent behaviors of heterobimetallic complexes of bis(salamo)-type ligand, herein we have designed and prepared a novel heterobimetallic complex $[\text{Cu}_2(\text{L})\text{Na}(\mu\text{-NO}_3)]\cdot\text{CH}_3\text{OH}\cdot\text{CHCl}_3$ derived from the bis(salamo)-type tetraoxime H_4L containing a naphthalenediol unit. The structural representation of H_4L is shown in Figure 1. Most importantly, the spectroscopic studies of the $\text{Cu}(\text{II})-\text{Na}(\text{I})$ complex were investigated.

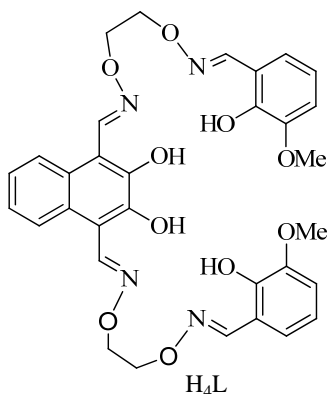


Figure 1. Structural representation of H_4L .

2. Results and Discussion

2.1. IR Spectra

The main FT-IR absorption bands characteristic for H_4L and its $\text{Cu}(\text{II})-\text{Na}(\text{I})$ complex from 500 to 4000 cm^{-1} regions are shown in Table 1.

Table 1. Main FT-IR absorption bands for H_4L and its $\text{Cu}(\text{II})-\text{Na}(\text{I})$ complex (cm^{-1}).

Compound	$\nu(\text{O}-\text{H})$	$\nu(\text{C}=\text{N})$	$\nu(\text{Ar}-\text{O})$	$\nu(\text{M}-\text{N})$
H_4L	3172	1634	1241	–
Complex	–	1618	1232	565

Generally, the typical $\text{O}-\text{H}$ stretching band is usually observed at the $3500\text{--}3100\text{ cm}^{-1}$ region. A broad band of medium intensity was found around 3172 cm^{-1} in the free ligand H_4L , this is an evidence for the stretching vibration of the $\text{O}-\text{H}$ groups. However, this band disappeared in the $\text{Cu}(\text{II})-\text{Na}(\text{I})$ complex. H_4L showed a typical $\text{C}=\text{N}$ stretching band occurring at 1634 cm^{-1} , while the $\text{Cu}(\text{II})-\text{Na}(\text{I})$ complex showed this band at 1618 cm^{-1} . In contrast to the free ligand H_4L it is moved to a lower wavenumber by 16 cm^{-1} due to coordination of the N atoms of the $\text{C}=\text{N}$ groups to the $\text{Cu}(\text{II})$ atoms [57]. This fact is also approved by the appearance of new bands within the wavenumber at 565 cm^{-1} due to $\nu(\text{Cu}(\text{II})-\text{N})$ vibrations. The characteristic absorption band of the $\text{Ar}-\text{O}$ group occurred at 1241 cm^{-1} in H_4L . However, the $\text{Ar}-\text{O}$ stretching band in the $\text{Cu}(\text{II})-\text{Na}(\text{I})$ complex was moved to a lower wavenumber at ca. 9 cm^{-1} , exhibiting that the $\text{M}-\text{O}$ bonds are formed between the metal atoms

and the methoxy and phenolic O atoms of H₄L [60]. The facts mentioned above are in agreement with the results of X ray diffraction.

2.2. UV-Vis Spectra

In this study, UV-Vis spectra of H₄L in CHCl₃:CH₃OH (1:1) ($c = 2.5 \times 10^{-5} \text{ mol L}^{-1}$) with its Cu(II)–Na(I) complex in CH₃OH:H₂O (10:1) ($c = 1 \times 10^{-3} \text{ mol L}^{-1}$) in freshly prepared solution are obtained in the range of 250–600 nm.

It can be seen from the absorption spectrum of H₄L, there are four continuous absorption peaks at about 269, 342, 360 and 378 nm [57]. The peak at 269 nm can be attributed to the π - π^* transition of the benzene rings while the other three peaks can be assigned to the π - π^* transition of the oxime groups [57,61].

In the titration experiment of the Cu(II)–Na(I) complex, the gradual addition of Cu(NO₃)₂ solution aroused the changes of absorption peaks. Compared to H₄L, the peaks are bathochromically shifted [62]. This fact mentioned above is owing to the coordination of the Cu(II) ion with H₄L. When 3 equiv of the Cu(II) ions were added to the solution of H₄L, the absorbance of the solution no longer changed. The spectral titration obviously revealed the formation of a 1:3 (ligand-to-Cu(II) ratio) Cu(II) complex (Figure 2a).

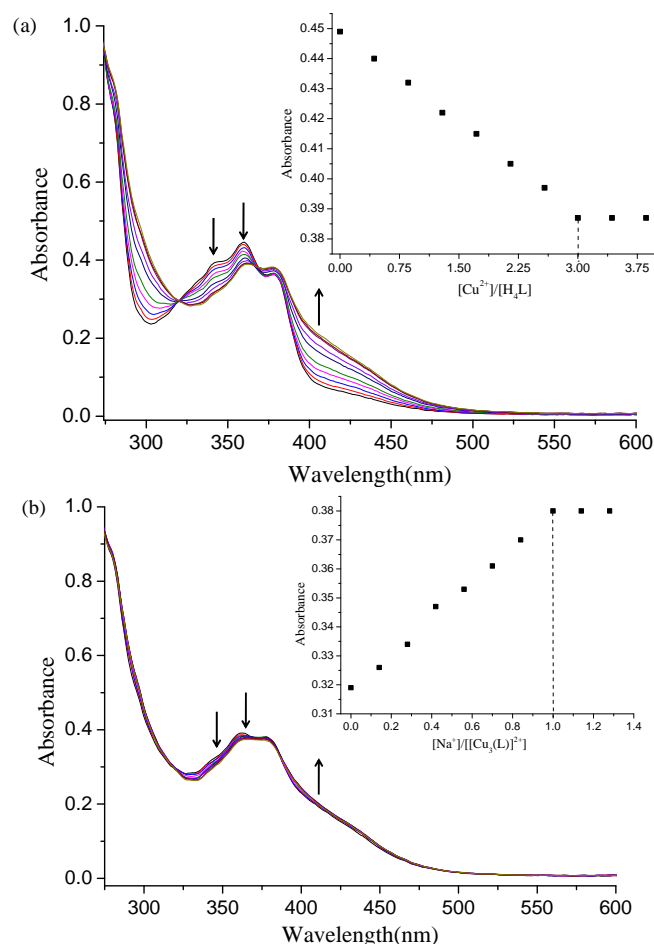


Figure 2. (a) UV-Vis spectral changes of H₄L ($2.5 \times 10^{-5} \text{ M}$) on addition of Cu(II) ions ($1.0 \times 10^{-3} \text{ M}$); (b) UV-Vis spectral changes of the $[\text{LCu}_3]^{2+}$ on addition of Na(I) ions ($1.0 \times 10^{-3} \text{ M}$).

What is more, the gradual additions of NaOAc solution were continuously added the above solution. Upon addition of 1 equiv of Na(I) ions, the solution absorbance basically remains stable. Clearly, the

spectral titration obviously indicated that the ratio of the replacement reaction stoichiometry is 1:1 and is depicted in Figure 2b.

2.3. Crystal Structure Description

The structure of the Cu(II)–Na(I) complex was characterized by X-ray crystallography, and is depicted in Figure 3.

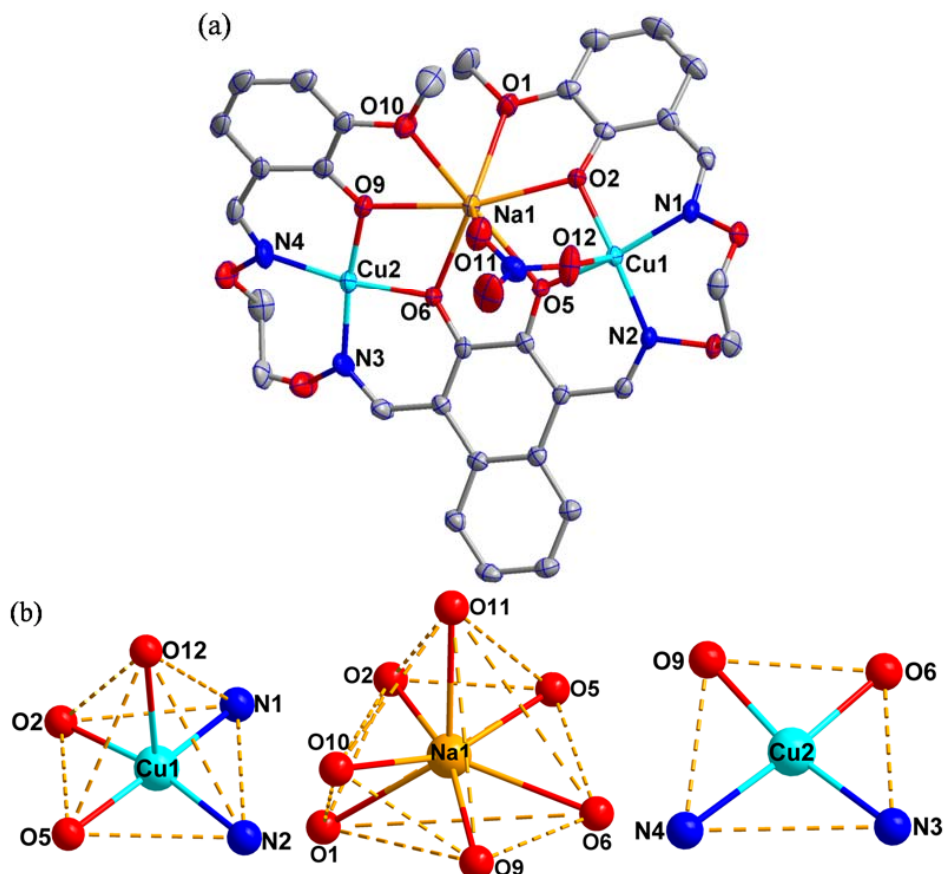


Figure 3. (a) Molecular structure of the Cu(II)–Na(I) complex (H atoms, crystallizing methanol and chloroform molecules are omitted for clarity, and thermal ellipsoids are drawn at the 30% probability level); (b) Coordination polyhedrons for Cu(II) and Na(I) atoms.

It is shown that the Cu(II)–Na(I) complex crystallizes in the monoclinic system with space group $P 2_1/n$ (Attempting to set the space group to $P 2_1/c$, the structure of the complex was not determined, which is determined by the different orientations chosen when determining the crystal cell. The structure of expected complex is obtained when the space group is set to $P 2_1/n$, and the bond lengths and angles are all within the expected ranges.) [63] and contains two Cu(II) atoms, one Na(I) atom, one completely deprotonated (L)^{4−} moiety, one μ -NO₃ ion, one crystallizing methanol and chloroform molecules, possessing a hetero-trinuclear structure. According to our design, the bis(salamo)-type ligand H₄L has an O₆ coordination sphere which is usually occupied by a larger radius metal ion [64]. Therefore, we consider the complex obtained to be a heterotrimeric Cu(II)–Na(I) complex and not sodium salt of the Cu(II) complex [65]. At the same time, it is shown that the ligand-to-metal (Cu(II) and Na(I)) ratio is 1:2:1. This structure in this paper is different from the structure reported earlier, in which the two Cu(II) atoms are located in N₂O₂ sites, and one Cu(II) atom is still bonded to a methanol molecule, while the other Cu(II) atom is bonded to one O atom of a μ -NO₃ ion. Finally, both Cu(II) atoms adopt five-coordinated and possess geometries of slightly distorted

square pyramid. The capped site is occupied by Br3 with the bond length (Na1–Br3, 2.765(3) Å) and the Na–O bond length is in the ranges of 2.324(2)–3.025(3) Å [17].

As shown in Figure 3, the N₂O₂ compartments of the fully deprotonated (L)^{4−} moiety are occupied by two Cu(II) atoms (Cu1 and Cu2), while the central Na(I) atom is located at O₆ cavity. The Cu1 atom is bonded to two N atoms (Cu1–N1, 2.002(3) and Cu1–N2, 1.950(3)) and two O atoms (Cu1–O2, 1.907(2) Å and Cu1–O5, 1.903(2) Å) of the ligand (L)^{4−} moiety forming the square base. Meantime, the Cu1 atom is also coordinated with one O atom (Cu1–O12, 2.462(3) Å) of a bidentate μ -NO₃ ion. The Cu1 atom is five-coordinated with geometry of a slightly distorted square pyramid, which was deduced by calculating the value of $\tau = 0.0058$ [66]. Interestingly, the Cu2 atom is coordinated to the N atoms (Cu2–N3, 1.944(3) Å and Cu2–N4, 1.981(3) Å) and O atoms (Cu2–O6, 1.909(2) Å and Cu2–O9, 1.907(3) Å) of the N₂O₂ site. Therefore, the Cu2 atom is four-coordinated and possesses a geometry of slightly distorted square planar. The Na(I) atom occupies central O₆ site (Na1–O1, 2.546(3) Å; Na1–O2, 2.388(3) Å; Na1–O5, 2.355(3) Å; Na1–O6, 2.454(3) Å; Na1–O9, 2.429(3) Å and Na1–O10, 2.475(3) Å) from four phenolic O and two methoxy O atoms of the ligand (L)^{4−} moiety [17]. Meanwhile, the Na(I) atom is still coordinated to one O atom (Na1–O11, 2.490(4)) of μ -NO₃ ion. In a word, the Na–O bond length is in the range of 2.355(3)–2.546(3) Å, which is in the regular range compared with previously reported data [17]. Therefore, according to our previous report, the Na–O bonds mentioned above could be regarded as coordination bonds. Finally, the Na(I) atom adopts seven-coordinated and possesses a geometry of slightly distorted single triangular prism. The crystallographic data and structure refinement parameters are summed in Table 2. Selected bond lengths and angles are summed in Table 3.

Table 2. Crystal and structure refinement data for the Cu(II)–Na(I) complex.

Empirical Formula	C ₃₄ H ₃₃ Cl ₃ Cu ₂ NaN ₅ O ₁₄
Formula weight	992.07
T (K)	154.89(10)
Radiation (Å)	Mo K α , 0.71073
Crystal system	Monoclinic
Space group	<i>P</i> 2 ₁ / <i>n</i>
<i>a</i> (Å)	15.8326(3)
<i>b</i> (Å)	11.4630(2)
<i>c</i> (Å)	21.7834(4)
α (°)	90
β (°)	98.135(2)
γ (°)	90
Volume (Å ³)	3913.68(14)
<i>Z</i>	4
<i>D_c</i> (g·cm ^{−3})	1.684
Absorption coefficient (mm ^{−1})	1.377
Θ range for data collection (°)	3.281 to 26.021
<i>F</i> (000)	2016
<i>h</i> / <i>k</i> / <i>l</i> (min, max)	−19,19/−14,14/−26,26
Crystal size (mm)	0.15 × 0.21 × 0.24
Reflections collected	16726/7694
Independent reflection	[<i>R</i> _{int} = 0.035]
<i>S</i>	7694
Data/restraints/parameters	1.033
Final <i>R</i> indices [<i>I</i> > 2 σ (<i>I</i>)] ^a	5555/54/581
<i>R</i> indices (all data) ^b	<i>R</i> ₁ = 0.0478
	<i>wR</i> ₂ = 0.0738

Table 3. Selected bond distances (Å) and angles (°) for the Cu(II)–Na(I) complex.

Bonds Lengths (Å)			Bonds Lengths (Å)		
Cu1-O2	1.907(2)	Cu1-O5	1.903(2)	Cu1-O12	2.462(3)
Cu1-N1	2.002(3)	Cu1-N2	1.949(3)	Cu2-O6	1.910(2)
Cu2-O9	1.907(3)	Cu2-N3	1.945(3)	Cu2-N4	1.980(3)
Na1-O1	2.547(3)	Na1-O2	2.389(3)	Na1-O5	2.356(3)
Na1-O6	2.453(3)	Na1-O9	2.428(3)	Na1-O10	2.475(3)
Na1-O11	2.492(4)				
Angle (°)			Angle (°)		
O1-Na1-O2	62.93(9)	O1-Na1-O5	114.77(9)	O1-Na1-O6	125.89(10)
O1-Na1-O9	100.91(9)	O1-Na1-O11	127.1(12)	O2-Na1-O5	65.17(9)
O2-Na1-O6	125.67(9)	O2-Na1-O9	163.84(9)	O2-Na1-O10	109.08(9)
O5-Na1-O6	64.19(9)	O5-Na1-O9	126.70(9)	O5-Na1-O10	158.77(12)
O6-Na1-O9	62.91(9)	O6-Na1-O10	125.25(9)	O6-Na1-O11	106.71(9)
O9-Na1-O10	64.01(10)	O9-Na1-O11	108.71(9)	O10-Na1-O11	78.44(12)

2.4. Supramolecular Interactions

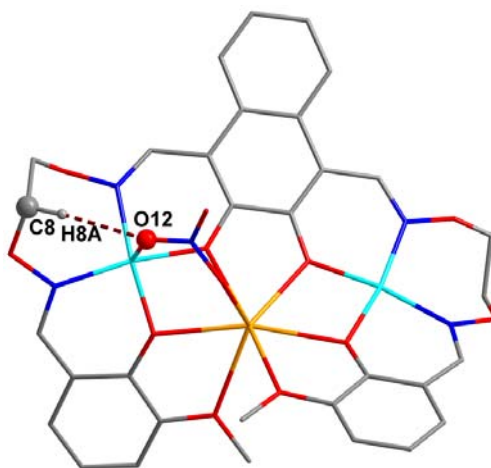
Single crystal determination showed that the Cu(II)–Na(I) complex forms a self-assembling infinite supra-molecular structure by C–H··· π and hydrogen bond interactions. The hydrogen bonds and C–H··· π stacking interactions are listed in Table 4.

Table 4. Hydrogen bondings (Å, deg) and C–H··· π stacking interactions of Cu(II)–Na(I) complex.

D–H···A	d(D–H)	d(H···A)	d(D···A)	\angle DHA
C8–H8A···O12	0.97	2.29	3.252(6)	171
O14–H14A···O12 ^{#1}	0.82	2.37	3.075(6)	144
O14–H14A···O13 ^{#1}	0.82	2.50	3.267(8)	157
C23–H23B···O13 ^{#1}	0.97	2.31	2.987(9)	126
C15–H15···Cg1 ^{#2}	0.96	2.79	3.473(5)	131

Symmetry codes: ^{#1} $x, 1 + y, z$; ^{#2} $1 - x, 1 - y, -z$; Cg1 for the Cu(II)–Na(I) complex is the centroid of C1–C6 atoms.

In the Cu(II)–Na(I) complex, there is one intra-molecular C8–H8A···O12 hydrogen bond, showing in Figure 4. As illustrated in Figure 5, an infinite 2D supra-molecular structure is interlinked via three pairs of inter-molecular O14–H14A···O12, O14–H14A···O13 and C23–H23B···O13 hydrogen bonds [67–75]. Especially, one significant C15–H15···Cg1 (C1–C6) (C–H··· π) interaction is constructed and shown in Figure 6.

**Figure 4.** Intra-molecular hydrogen bond interactions of the Cu(II)–Na(I) complex.

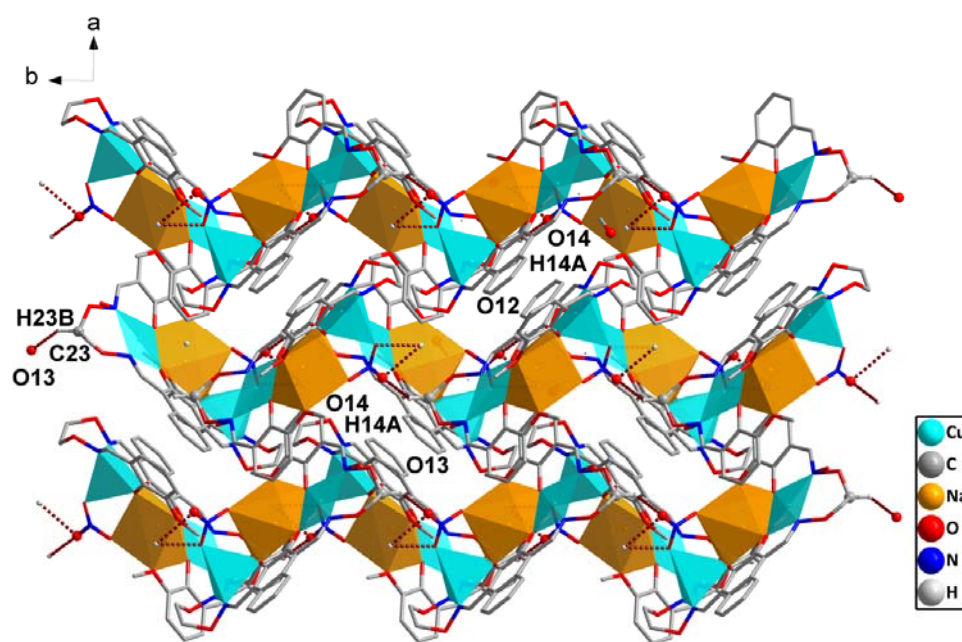


Figure 5. 2D supra-molecular structure by inter-molecular O-H...O and C-H...O interactions in the Cu(II)–Na(I) complex.

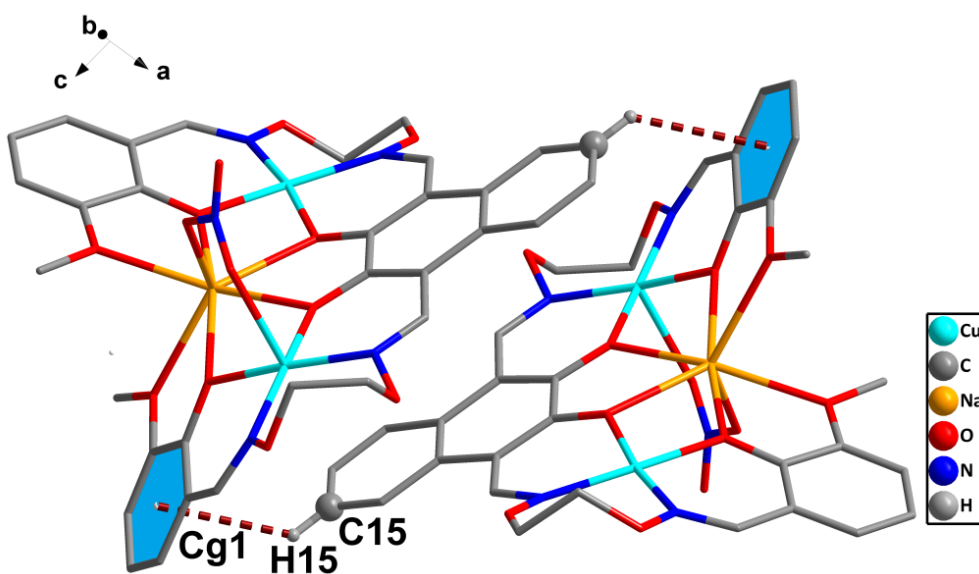


Figure 6. Intermolecular C-H... π interactions of the Cu(II)–Na(I) complex.

2.5. Fluorescence Spectra

The emission spectra of H₄L in CHCl₃:CH₃OH (1:1) ($c = 2.5 \times 10^{-5} \text{ mol L}^{-1}$) solution and its Cu(II)–Na(I) complex in CH₃OH ($c = 1.0 \times 10^{-5} \text{ mol L}^{-1}$) were determined at room temperature.

As shown in Figure 7, the ligand H₄L exhibited one relatively strong emission at 440 nm upon excitation at 330 nm, which should be attributed to the intra-ligand π – π^* transition [67]. In comparison with the H₄L, fluorescent property study of the Cu(II)–Na(I) complex is shown that the fluorescent intensity weakens markedly, exhibiting a broad peak with maximum emission at 429 nm upon excitation at 330 nm. That hypsochromic-shift phenomenon can explain the complexation of H₄L and metal ions (Cu(II) and Na(I)), which is attributed to ligand-to-metal charge transfer (LMCT) [68].

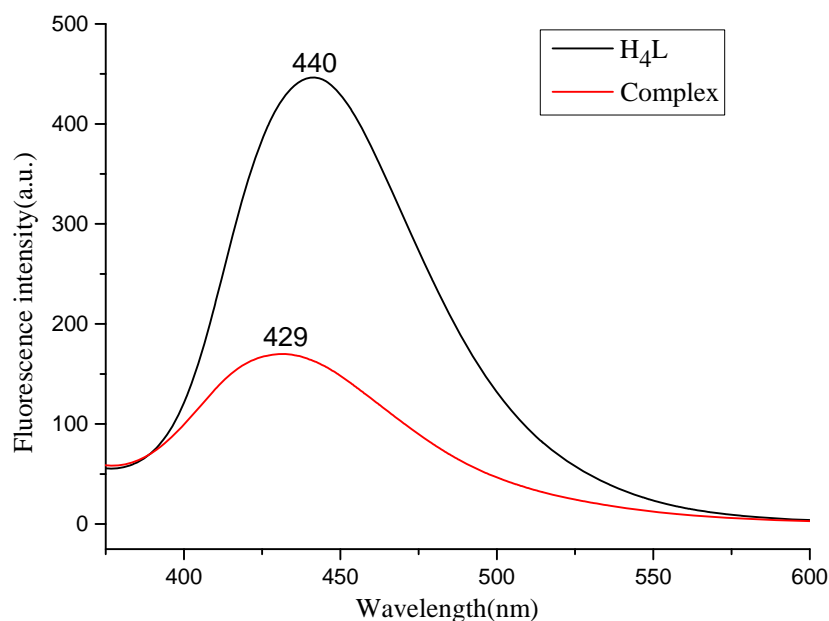


Figure 7. Emission spectra of H₄L and its Cu(II)–Na(I) complex.

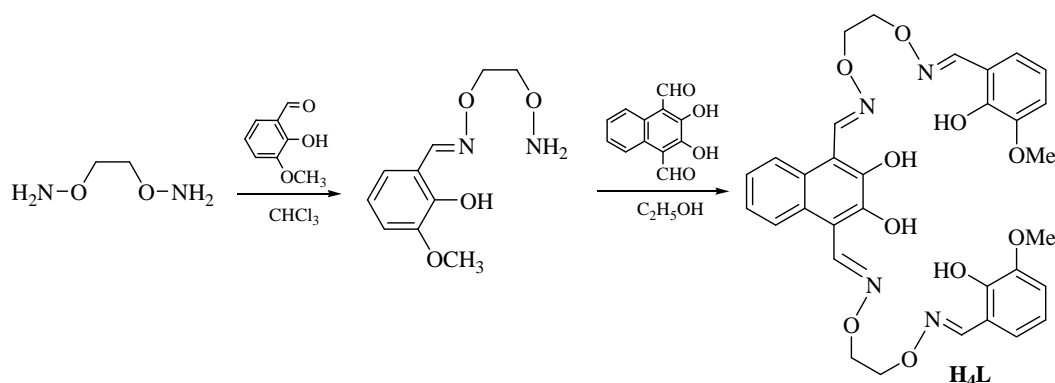
3. Experimental Section

3.1. Materials and Methods

2-Hydroxy-3-methoxybenzaldehyde (99%), pyridinium chlorochromate (98%), methyl trioctyl ammonium chloride (90%) and borontribromide (99.9%) were bought from Alfa Aesar (New York, NY, USA). Hydrobromic acid 33 wt % solution in acetic acid was purchased from J&K Scientific Ltd. (Beijing, China). All chemicals and solvents used for the synthesis were of the best available analytical reagent grade, without further purification in the preparation of the free ligand and its complex. Elemental analyses for C, H, and N were carried out using a GmbH Vario EL V3.00 automatic elemental analysis instrument (Elementar, Berlin, Germany). Elemental analyses for Cu and Na atoms were detected with an IRIS ER/S-WP-1 ICP atomic emission spectrometer (IRIS, Elementar, Berlin, Germany). IR spectra were measured on a VERTEX70 FT-IR spectrophotometer (Bruker, Billerica, MA, USA), with samples prepared as KBr (500–4000 cm⁻¹) pellets. Melting points were recorded on use of a microscopic melting point apparatus made in Beijing Taike Instrument Limited Company and were uncorrected (Beijing, China). UV-Vis absorption spectra were recorded on a Shimadzu UV-3900 spectrometer (Hitachi, Shimadzu, Tokyo, Japan). The fluorescence spectra were taken on Hitachi F-7000 spectrometer (Hitachi, Tokyo, Japan). X-ray single crystal structure determinations were carried out on a Super Nova Dual (Cu at zero) Eos four-circle diffractometer (Bruker, Billerica, MA, USA).

3.2. Synthesis of H₄L

The main reaction steps involved in the synthesis of H₄L was gained via reacting 2,3-dihydroxynaphthalene-1,4-dicarbaldehyde with 3-methoxysalicylaldehyde. 2,3-Dihydroxynaphthalene-1,4-dicarbaldehyde and 2-[O-(1-ethyloxyamide)]oxime-6-methoxyphenol were prepared according to an analogous method [28,57–59]. The synthesis of H₄L is given in Scheme 1.



Scheme 1. Synthetic route to H₄L.

H₄L was prepared according to the previously reported method [28,57–59]. Yield: 60.2%. m.p. 170–171 °C. Anal. Calcd. (%) for C₃₂H₃₂N₄O₁₀ (632.42): C, 60.75; H, 5.10; N, 8.86. Found (%): C, 60.93; H, 5.23; N, 8.74. ¹H-NMR (400 MHz, CDCl₃) δ 11.03 (s, 2H), 9.82 (s, 2H), 9.14 (s, 2H), 8.29 (s, 2H), 7.97 (q, *J* = 3.2 Hz, 2H), 7.41 (q, *J* = 6.0, 2.9 Hz, 2H), 7.06–6.68 (m, 6H), 4.58 (t, 8H), 3.89 (s, 6H). UV-Vis [in methanol/chloroform (1:1)], λ_{max} (nm) [2.5 × 10^{−5} M]: 269, 342, 360, 378.

3.3. Synthesis of the Cu(II)–Na(I) Complex

A mixture solution of Cu(NO₃)₂·2H₂O (4.82 mg, 0.02 mmol) in methanol (2 mL) and NaOAc (0.82 mg, 0.01 mmol) in methanol (2 mL) was added to a stirring solution of H₄L (6.32 mg, 0.01 mmol) in chloroform (2 mL). The color of the mixing solution immediately turned dark green. The mixture was filtered, and the filtrate was allowed to stay for slow evaporation. After about three weeks, clear light green single-crystals suitable for X-ray diffraction studies were gained. Yield: 40.3%. Anal. Calcd. (%) for C₃₄H₃₃Cl₃Cu₂NaN₅O₁₄ (992.07): C, 41.16; H, 3.35; N, 7.06; Cu, 12.81; Na, 2.32. Found (%): C, 41.33; H, 3.49; N, 6.88; Cu, 12.64; Na, 2.17. UV-Vis [in methanol/H₂O (10:1)], λ_{max} (nm) [1.0 × 10^{−3} M]: 350, 369, 382.

3.4. Crystal Structure Determination and Refinement

Single crystal of dimensions 0.15 × 0.21 × 0.24 mm for the heterotrinary Cu(II)–Na(I) complex was mounted on a glass rod. The crystal data were collected with a Super Nova (Dual, Cu at zero, Eos) diffractometer with graphite monochromated Mo K α radiation (λ = 0.71073 Å) at 154.89(10) K. Multiscan absorption corrections were applied. The structure was solved by direct methods and refined anisotropically using full-matrix least-squares methods on *F*² with the SHELX-2014 program package. Nonhydrogen atoms of the compound were refined with anisotropic temperature parameters. The positions of H atoms were calculated and isotropically fixed in the final refinement.

Supplementary crystallographic data have been deposited at Cambridge Crystallographic Data Centre (CCDC No. 1815945) and can be gained free of charge via www.ccdc.cam.ac.uk/conts/retrieving.html.

4. Conclusions

Overall, we have designed and synthesized a novel heterobimetallic Cu(II)–Na(I) complex derived from a symmetric bis(salamo)-type ligand H₄L. X-ray crystallographic investigation of the heterotrinary Cu(II)–Na(I) complex revealed there is a 1:2:1 ligand-to-metal (Cu(II) and Na(I)) ratio. The Cu1 atom is five-coordinated and possesses the geometry of slightly distorted square pyramid and the Cu2 atom is four-coordinated and possesses the geometry of square planar. The Na(I) atom adopts seven-coordinated with a slightly distorted single triangular prism geometry. The UV-Vis titration experiment clearly displayed the coordination ratio between the ligand H₄L and the Cu(II) and Na(I)

ions. The fluorescence spectra showed the complex possesses a significant fluorescent quenching, and exhibited a hypsochromic-shift compared with the ligand H₄L.

Supplementary Materials: Supplementary materials are available online.

Author Contributions: W.-K.D. supervised the project and contributed materials/reagents/analysis tools; X.-Y.D., Z.-L.W., H.-R.M. and H.Z. performed the experiments; W.-K.D. and Q.Z. wrote the manuscript.

Acknowledgments: This work was supported by the National Natural Science Foundation of China (21761018) and the Program for Excellent Team of Scientific Research in Lanzhou Jiaotong University (201706), both of which are gratefully acknowledged.

Conflicts of Interest: The authors declare no conflict of interest.

References

1. Sun, S.S.; Stern, C.L.; Nguyen, S.T.; Hupp, J.T. Directed assembly of transition-metal-coordinated molecular loops and square from Salen-type components. Examples of metalation controlled structural conversion. *J. Am. Chem. Soc.* **2004**, *126*, 6314–6326. [[CrossRef](#)] [[PubMed](#)]
2. Shu, Y.B.; Liu, W.S. Luminescent chiral Eu(III) complexes with enantiopurebis(1*H*-pyridin-2-one)salen ligands. *Polyhedron* **2015**, *102*, 293–296. [[CrossRef](#)]
3. Zhao, L.; Wang, L.; Sun, Y.X.; Dong, W.K.; Tang, X.L.; Gao, X.H. A supramolecular copper(II) complex bearing salen-type bisoxime ligand: Synthesis, structural characterization and thermal property. *Synth. React. Inorg. Met.-Org. Nano-Met. Chem.* **2012**, *42*, 1303–1308. [[CrossRef](#)]
4. Ma, X.; Jiao, J.M.; Yang, J.; Huang, X.B.; Cheng, Y.X.; Zhu, C.J. Large stokes shift chiral polymers containing (*R,R*)-salen-based binuclear boron complex: Synthesis, characterization, and fluorescence properties. *Polyhedron* **2012**, *53*, 3894–3899. [[CrossRef](#)]
5. Sun, Y.X.; Zhang, S.T.; Ren, Z.L.; Dong, X.Y.; Wang, L. Synthesis, characterization, and crystal structure of a new supramolecular Cd^{II} complex with halogen-substituted salen-type bisoxime. *Synth. React. Inorg. Met.-Org. Nano-Met. Chem.* **2013**, *43*, 995–1000. [[CrossRef](#)]
6. Liu, P.P.; Sheng, L.; Song, X.Q.; Xu, W.Y.; Liu, Y.A. Synthesis, structure and magnetic properties of a new one dimensional manganese coordination polymer constructed by a new asymmetrical ligand. *Inorg. Chim. Acta* **2015**, *434*, 252–257. [[CrossRef](#)]
7. Sun, Y.X.; Gao, X.H. Synthesis, characterization, and crystal structure of a new Cu^{II} complex with salen-type ligand. *Synth. React. Inorg. Met.-Org. Nano-Met. Chem.* **2011**, *41*, 973–978. [[CrossRef](#)]
8. Sun, Y.X.; Xu, L.; Zhao, T.H.; Liu, S.H.; Liu, G.H.; Dong, X.T. Synthesis and crystal structure of a 3D supramolecular copper(II) complex with 1-(3-[(*E*)-3-bromo-5-chloro-2-hydroxybenzylidene]amino)phenyl) ethanoneoxime. *Synth. React. Inorg. Met.-Org. Nano-Met. Chem.* **2013**, *43*, 509–513. [[CrossRef](#)]
9. Chin, T.K.; Endud, S.; Jamil, S.; Budagumpi, S.; Lintang, H.O. Oxidative dimerization of o-aminophenol by heterogeneous mesoporous material modified with biomimetic salen-type copper(II) complex. *Catal. Lett.* **2013**, *143*, 282–288. [[CrossRef](#)]
10. Li, X.Y.; Chen, L.; Gao, L.; Zhang, Y.; Akogun, S.F.; Dong, W.K. Syntheses, crystal structures and catalytic activities of two solvent-induced homotrinnuclear Co(II) complexes with a naphthalenediol-based bis(salamo)-type tetraoxime ligand. *RSC Adv.* **2017**, *7*, 35905–35916. [[CrossRef](#)]
11. Chai, L.Q.; Wang, G.; Sun, Y.X.; Dong, W.K.; Zhao, L.; Gao, X.H. Synthesis, crystal structure, and fluorescence of an unexpected dialkoxo-bridged dinuclear copper(II) complex with bis(salen)-type tetraoxime. *J. Coord. Chem.* **2012**, *65*, 1621–1631. [[CrossRef](#)]
12. Chai, L.Q.; Huang, J.J.; Zhang, H.S.; Zhang, Y.L.; Zhang, J.Y.; Li, Y.X. An unexpected cobalt(III) complex containing a Schiff base ligand: Synthesis, crystal structure, spectroscopic behavior, electrochemical property and SOD-like activity. *Spectrochim. Acta Part A* **2014**, *131*, 526–531. [[CrossRef](#)] [[PubMed](#)]
13. Chai, L.Q.; Liu, G.; Zhang, J.Y.; Huang, J.J.; Tong, J.F. Synthesis, crystal structure, fluorescence, electrochemical property, and SOD-like activity of an unexpected nickel(II) complex with a quinazoline-type ligand. *J. Coord. Chem.* **2013**, *66*, 3926–3938. [[CrossRef](#)]
14. Chai, L.Q.; Zhang, H.S.; Huang, J.J.; Zhang, Y.L. An unexpected Schiff base-type Ni(II) complex: Synthesis, crystal structures, fluorescence, electrochemical property and SOD-like activities. *Spectrochim. Acta Part A* **2015**, *137*, 661–669. [[CrossRef](#)] [[PubMed](#)]

15. Chai, L.Q.; Tang, L.J.; Chen, L.C.; Huang, J.J. Structural, spectral, electrochemical and DFT studies of two mononuclear manganese(II) and zinc(II) complexes. *Polyhedron* **2017**, *122*, 228–240. [[CrossRef](#)]
16. Chai, L.Q.; Zhang, K.Y.; Tang, L.J.; Zhang, J.Y.; Zhang, H.S. Two mono- and dinuclear Ni(II) complexes constructed from quinazoline-type ligands: Synthesis, X-ray structures, spectroscopic, electrochemical, thermal, and antimicrobial studies. *Polyhedron* **2017**, *130*, 100–107. [[CrossRef](#)]
17. Chen, L.; Dong, W.K.; Zhang, H.; Zhang, Y.; Sun, Y.X. Structural variation and luminescence properties of tri- and dinuclear Cu^{II} and Zn^{II} complexes constructed from a naphthalenediol-based bis(Salamo)-type ligand. *Cryst. Growth Des.* **2017**, *17*, 3636–3648. [[CrossRef](#)]
18. Dong, X.Y.; Li, X.Y.; Liu, L.Z.; Zhang, H.; Ding, Y.J.; Dong, W.K. Tri- and hexanuclear heterometallic Ni(II)–M(II) (M = Ca, Sr and Ba) bis(salamo)-type complexes: Synthesis, structure and fluorescence properties. *RSC Adv.* **2017**, *7*, 48394–48403. [[CrossRef](#)]
19. Song, X.Q.; Peng, Y.J.; Chen, G.Q.; Wang, X.R.; Liu, P.P.; Xu, W.Y. Substituted group-directed assembly of Zn(II) coordination complexes based on two new structural related pyrazolone based Salen ligands: Syntheses, structures and fluorescence properties. *Inorg. Chim. Acta* **2015**, *427*, 13–21. [[CrossRef](#)]
20. Wang, P.; Zhao, L. An infinite 2D supramolecular cobalt(II) complex based on an asymmetric salamo-type ligand: Synthesis, crystal structure, and spectral properties. *Synth. React. Inorg. Met.-Org. Nano-Met. Chem.* **2016**, *46*, 1095–1101. [[CrossRef](#)]
21. Lee, S.H.; Shin, N.; Kwak, S.W.; Hyun, K.; Woo, W.H.; Lee, J.H.; Hwang, H.; Kim, M.; Lee, J.; Kim, Y.; et al. Intriguing indium-salen complexes as multicolor luminophores. *Inorg. Chem.* **2017**, *56*, 2621–2626. [[CrossRef](#)] [[PubMed](#)]
22. Tao, C.H.; Ma, J.C.; Zhu, L.C.; Zhang, Y.; Dong, W.K. Heterobimetallic 3d–4f Zn(II)–Ln(III) (Ln = Sm, Eu, Tb and Dy) complexes with a N₂O₄ bisoxime chelate ligand and a simple auxiliary ligand Py: Syntheses, structures and luminescence properties. *Polyhedron* **2017**, *128*, 38–45. [[CrossRef](#)]
23. Abe, A.M.M.; Helaja, J.; Koskinen, A.M.P. Novel crown ether and Salen metal chelation driven molecular pincers. *Org. Lett.* **2006**, *8*, 4537–4540. [[CrossRef](#)] [[PubMed](#)]
24. Dong, W.K.; Ma, J.C.; Dong, Y.J.; Zhao, L.; Zhu, L.C.; Sun, Y.X.; Zhang, Y. Two hetero-trinuclear Zn(II)–M(II) (M = Sr, Ba) complexes based on metallohost of mononuclear Zn(II) complex: Syntheses, structures and fluorescence properties. *J. Coord. Chem.* **2016**, *69*, 3231–3241. [[CrossRef](#)]
25. Hao, J.; Li, X.Y.; Zhang, Y.; Dong, W.K. A reversible bis(salamo)-based fluorescence sensor for selective detection of Cd²⁺ in water-containing systems and food samples. *Materials* **2018**, *11*, 523. [[CrossRef](#)] [[PubMed](#)]
26. Wang, L.; Ma, J.C.; Dong, W.K.; Zhu, L.C.; Zhang, Y. A novel self-assembled nickel(II)–cerium(III) heterotetranuclear dimer constructed from N₂O₂-type bisoxime and terephthalic acid: Synthesis, structure and photophysical properties. *Z. Anorg. Allg. Chem.* **2016**, *642*, 834–839. [[CrossRef](#)]
27. Ömer, S.; Ümmühan, Ö.Ö.; Nurgul, S.; Burcu, A.; Musa, S.; Tuncay, T.; Zeynel, S. A highly selective and sensitive chemosensor derived coumarin-thiazole for colorimetric and fluorimetric detection of CN[−] ion in DMSO and aqueous solution: Synthesis, sensing ability, Pd(II)/Pt(II) complexes and theoretical studies. *Tetrahedron* **2016**, *72*, 5843–5852.
28. Zhang, H.; Dong, W.K.; Zhang, Y.; Akogun, S.F. Naphthalenediol-based bis(Salamo)-type homo- and heterotrimeric cobalt(II) complexes: Syntheses, structures and magnetic properties. *Polyhedron* **2017**, *133*, 279–293. [[CrossRef](#)]
29. Wu, H.L.; Bai, Y.C.; Zhang, Y.H.; Li, Z.; Wu, M.C.; Chen, C.Y.; Zhang, J.W. Synthesis, crystal structure, antioxidation and DNA-binding properties of a dinuclear copper(II) complex with bis(*N*-salicylidene)-3-oxapentane-1,5-diamine. *J. Coord. Chem.* **2014**, *67*, 3054–3066. [[CrossRef](#)]
30. Chen, C.Y.; Zhang, J.W.; Zhang, Y.H.; Yang, Z.H.; Wu, H.L.; Pan, G.L.; Bai, Y.C. Gadolinium(III) and dysprosium(III) complexes with a Schiff base bis(*N*-salicylidene)-3-oxapentane-1,5-diamine: Synthesis, characterization, antioxidation, and DNA-binding studies. *J. Coord. Chem.* **2015**, *68*, 1054–1071. [[CrossRef](#)]
31. Wu, H.L.; Bai, Y.H.; Zhang, Y.H.; Pan, G.L.; Kong, J.; Shi, F.R.; Wang, X.L. Two lanthanide (III) complexes based on the Schiff base *N,N'*-bis(salicylidene)-1,5-diamino-3-oxapentane: Synthesis, characterization, DNA-binding properties, and antioxidation. *Z. Anorg. Allg. Chem.* **2014**, *640*, 2062–2071. [[CrossRef](#)]

32. Wu, H.L.; Pan, G.L.; Wang, H.; Wang, X.L.; Bai, Y.C.; Zhang, Y.H. Study on synthesis, crystal structure, antioxidant and DNA-binding of mono-, di- and poly-nuclear lanthanides complexes with bis(*N*-salicylidene)-3-oxapentane-1,5-diamine. *J. Photochem. Photobiol. B* **2014**, *135*, 33–43. [[CrossRef](#)] [[PubMed](#)]
33. Wu, H.L.; Pan, G.L.; Bai, Y.C.; Wang, H.; Kong, J.; Shi, F.; Zhang, Y.H.; Wang, X.L. Preparation, structure, DNA-binding properties, and antioxidant activities of a homodinuclear erbium(III) complex with a pentadentate Schiff base ligand. *J. Chem. Res.* **2014**, *38*, 211–217. [[CrossRef](#)]
34. Wu, H.L.; Wang, H.; Wang, X.L.; Pan, G.L.; Shi, F.R.; Zhang, Y.H.; Bai, Y.C.; Kong, J. V-shaped ligand bis(2-benzimidazolymethyl)amine containing three copper(II) ternary complexes: Synthesis, structure, DNA-binding properties and antioxidant activity. *New J. Chem.* **2014**, *38*, 1052–1061. [[CrossRef](#)]
35. Wu, H.L.; Wang, C.P.; Wang, F.; Peng, H.P.; Zhang, H.; Bai, Y.C. A new manganese (III) complex from bis(5-methylsalicylaldehyde)-3-oxapentane-1,5-diamine: Synthesis, characterization, antioxidant activity and luminescence. *J. Chin. Chem. Soc.* **2015**, *62*, 1028–1034. [[CrossRef](#)]
36. Wu, H.L.; Pan, G.L.; Bai, Y.C.; Wang, H.; Kong, J.; Shi, F.R.; Zhang, Y.H.; Wang, X.L. Synthesis, structure, antioxidation, and DNA-binding studies of a binuclear ytterbium(III) complex with bis(*N*-salicylidene)-3-oxapentane-1,5-diamine. *Res. Chem. Intermed.* **2015**, *41*, 3375–3388. [[CrossRef](#)]
37. Wang, F.; Xu, Y.L.; Aderinto, S.O.; Peng, H.P.; Zhang, H.; Wu, H.L. A new highly effective fluorescent probe for Al³⁺ ions and its application in practical samples. *J. Photochem. Photobiol. A* **2017**, *332*, 273–282. [[CrossRef](#)]
38. Akine, S.; Piao, S.; Miyashita, M.; Nabeshima, T. Cage-like tris(salen)-type metallocryptand for cooperative guest recognition. *Tetrahedron Lett.* **2013**, *54*, 6541–6544. [[CrossRef](#)]
39. Dong, Y.J.; Li, X.L.; Zhang, Y.; Dong, W.K. A highly selective visual and fluorescent sensor for Pb²⁺ and Zn²⁺ and crystal structure of Cu²⁺ complex based on a novel single-armed salamo-type bisoxime. *Supramol. Chem.* **2017**, *29*, 518–527. [[CrossRef](#)]
40. Dong, W.K.; Ma, J.C.; Dong, Y.J.; Zhu, L.C.; Zhang, Y. Di- and tetranuclear heterometallic 3d–4f cobalt(II)–lanthanide(III) complexes derived from a hexadentate bisoxime: Syntheses, structures and magnetic properties. *Polyhedron* **2016**, *115*, 228–235. [[CrossRef](#)]
41. Zhou, J.J.; Song, X.Q.; Liu, Y.A.; Wang, X.L. Substituent-tuned structure and luminescence sensitizing towards Al³⁺ based on phenoxy bridged dinuclear Eu^{III} complexes. *RSC Adv.* **2017**, *7*, 25549–25559. [[CrossRef](#)]
42. Chakraborty, A.; Bag, P.; Goura, J.; Bar, A.K.; Sutter, J.-P.; Chandrasekhar, V. Chair-shaped Mn^{II}₂Ln^{III}₄ (Ln = Gd, Tb, Dy, Ho) heterometallic complexes assembled from a tricompartamental aminobenzohydrazide ligand. *Cryst. Growth Des.* **2015**, *15*, 848–857. [[CrossRef](#)]
43. Liu, Y.A.; Wang, C.Y.; Zhang, M.; Song, X.Q. Structures and magnetic properties of cyclic heterometallic tetranuclear clusters. *Polyhedron* **2017**, *127*, 278–286. [[CrossRef](#)]
44. Dong, W.K.; Ma, J.C.; Zhu, L.C.; Zhang, Y. Self-assembled zinc(II)-lanthanide(III) heteromultinuclear complexes constructed from 3-MeOsalamo ligand: Syntheses, structures and luminescent properties. *Cryst. Growth Des.* **2016**, *16*, 6903–6914. [[CrossRef](#)]
45. Dong, W.K.; Ma, J.C.; Zhu, L.C.; Zhang, Y. Nine self-assembled nickel(II)-lanthanide(III) heterometallic complexes constructed from a Salamo-type bisoxime and bearing a N- or O-donor auxiliary ligand: Syntheses, structures and magnetic properties. *New J. Chem.* **2016**, *40*, 6998–7010. [[CrossRef](#)]
46. Liu, P.P.; Wang, C.Y.; Zhang, M.; Song, X.Q. Pentanuclear sandwich-type Zn^{II}-Ln^{III} clusters based on a new salen-like salicylamide ligand: Structure, near-infrared emission and magnetic properties. *Polyhedron* **2017**, *129*, 133–140. [[CrossRef](#)]
47. Li, G.; Hao, J.; Liu, L.Z.; Zhou, W.M.; Dong, W.K. Syntheses, crystal structures and thermal behaviors of two supramolecular salamo-type cobalt(II) and zinc(II) complexes. *Crystals* **2017**, *7*, 217.
48. Wang, B.J.; Dong, W.K.; Zhang, Y.; Akogun, S.F. A novel relay-sensor for highly sensitive and selective detection of Zn²⁺/Pic[−] and fluorescence on/off switch response of H⁺/OH[−]. *Sens. Actuators B* **2017**, *247*, 254–264. [[CrossRef](#)]
49. Dong, W.K.; Li, G.; Wang, Z.K.; Dong, X.Y. A novel trinuclear cobalt(II) complex derived from an asymmetric salamo-type N₂O₃ bisoxime chelate ligand: Synthesis, structure and optical properties. *Spectrochim. Acta Part A* **2014**, *133*, 340–347. [[CrossRef](#)] [[PubMed](#)]
50. Dong, X.Y.; Gao, L.; Wang, F.; Zhang, Y.; Dong, W.K. Tri- and mono-nuclear zinc(II) complexes based on half- and mono-salamo chelating ligands. *Crystals* **2017**, *7*, 267. [[CrossRef](#)]

51. Yu, B.; Li, C.Y.; Sun, Y.X.; Jia, H.R.; Guo, J.Q.; Li, J. A new azine derivative colorimetric and fluorescent dual-channel probe for cyanide detection. *Spectrochim. Acta Part A* **2017**, *184*, 249–254. [[CrossRef](#)] [[PubMed](#)]
52. Dong, W.K.; Lan, P.F.; Zhou, W.M.; Zhang, Y. Salamo-type trinuclear and tetranuclear cobalt(II) complexes based on a new asymmetry salamo-type ligand: Syntheses, crystal structures, and fluorescence. *J. Coord. Chem.* **2016**, *69*, 1–22. [[CrossRef](#)]
53. Hao, J.; Liu, L.Z.; Dong, W.K.; Zhang, J.; Zhang, Y. Three multinuclear Co(II), Zn(II) and Cd(II) complexes based on a single-armed salamo-type bisoxime: Syntheses, structural characterizations and fluorescent properties. *J. Coord. Chem.* **2017**, *70*, 1936–1952. [[CrossRef](#)]
54. Wang, F.; Gao, L.; Zhao, Q.; Zhang, Y.; Dong, W.K.; Ding, Y.J. A highly selective fluorescent chemosensor for CN[−] based on a novel bis(salamo)-type tetraoxime ligand. *Spectrochim. Acta Part A* **2018**, *190*, 111–115. [[CrossRef](#)] [[PubMed](#)]
55. Gao, L.; Wang, F.; Zhao, Q.; Zhang, Y.; Dong, W.K. Mononuclear Zn(II) and trinuclear Ni(II) complexes derived from a coumarin-containing N₂O₂ ligand: Syntheses, crystal structures and fluorescence properties. *Polyhedron* **2018**, *139*, 7–16. [[CrossRef](#)]
56. Dong, W.K.; Du, W.; Zhang, X.Y.; Li, G.; Dong, X.Y. Synthesis, crystal structure and spectral properties of a supramolecular trinuclear nickel(II) complex with 5-methoxy-4'-bromo-2,2'-(ethylenedioxybis(nitrilomethylidyne)diphenol. *Spectrochim. Acta Part A* **2014**, *132*, 588–593. [[CrossRef](#)] [[PubMed](#)]
57. Dong, W.K.; Zheng, S.S.; Zhang, J.T.; Zhang, Y.; Sun, Y.X. Luminescent properties of heterotrinnuclear 3d–4f complexes constructed from a naphthalenediol-based acyclic bis(salamo)-type ligand. *Spectrochim. Acta Part A* **2017**, *184*, 141–150. [[CrossRef](#)] [[PubMed](#)]
58. Hao, J.; Li, L.H.; Zhang, J.T.; Akogun, S.F.; Wang, L.; Dong, W.K. Four homo- and hetero-bimetallic 3d/3d–2s complexes constructed from a naphthalenediol-based acyclic bis(salamo)-type tetraoxime ligand. *Polyhedron* **2017**, *134*, 1–10. [[CrossRef](#)]
59. Pu, L.M.; Zhao, Q.; Liu, L.Z.; Zhang, H.; Long, H.T.; Dong, W.K. Synthesis and fluorescence properties of a new heterotrinnuclear Co(II)–Ce(III) complex constructed from a bis(salamo)-type tetraoxime ligand. *Molecules* **2018**, *23*, 804. [[CrossRef](#)] [[PubMed](#)]
60. Dong, Y.J.; Ma, J.C.; Zhu, L.C.; Dong, W.K.; Zhang, Y. Four 3d–4f heteromultinuclear zinc(II)–lanthanide(III) complexes constructed from a distinct hexadentate N₂O₂-type ligand: Syntheses, structures and luminescence properties. *J. Coord. Chem.* **2017**, *70*, 103–115. [[CrossRef](#)]
61. Akine, S.; Sairenji, S.; Taniguchi, T.; Nabeshima, T. Stepwise helicity inversions by multisequential metal exchange. *J. Am. Chem. Soc.* **2013**, *135*, 12948–12951. [[CrossRef](#)] [[PubMed](#)]
62. Wang, L.; Li, X.Y.; Zhao, Q.; Li, L.H.; Dong, W.K. Fluorescence properties of heterotrinnuclear Zn(II)–M(II) (M = Ca, Sr and Ba) bis(salamo)-type complexes. *RSC Adv.* **2017**, *7*, 48730–48737. [[CrossRef](#)]
63. Dong, W.K.; Li, L.; Sun, Y.X.; Tong, J.F.; Wu, J.C. Syntheses, structures, and properties of 3,3'-dimethoxy-2,2'-(1,3-propylene)dioxybis(nitrilomethylidyne) diphenol and its Ni(II) cluster. *Synth. React. Inorg. Met.-Org. Nano-Met. Chem.* **2012**, *42*, 716–724. [[CrossRef](#)]
64. Akine, S.; Taniguchi, T.; Saiki, T.; Nabeshima, T. Ca²⁺- and Ba²⁺-selective receptors based on site-selective transmetalation of multinuclear polyoxime-zinc(II) complexes. *J. Am. Chem. Soc.* **2005**, *127*, 540–541. [[CrossRef](#)] [[PubMed](#)]
65. Akine, S.; Taniguchi, T.; Nabeshima, T. Helical metallohost-guest complexes via site-selective transmetalation of homotrinnuclear complexes. *J. Am. Chem. Soc.* **2006**, *128*, 15765–15774. [[CrossRef](#)] [[PubMed](#)]
66. Addison, A.W.; Nagaswara, R.T.; Reedijk, J.; Van Rijn, J.; Verschoor, G.C. Synthesis, structure, and spectroscopic properties of copper(II) compounds containing nitrogen-sulphur donor ligands; The crystal and molecular structure of aqua[1,7-bis(N-methylbenzimidazol-2'-yl)-2,6-dithiaheptane]copper(II) perchlorate. *J. Chem. Soc. Dalton Trans.* **1984**, 1349–1356. [[CrossRef](#)]
67. Xu, L.; Zhu, L.C.; Ma, J.C.; Zhang, Y.; Zhang, J.; Dong, W.K. Syntheses, structures and spectral properties of mononuclear Cu^{II} and dimeric Zn^{II} complexes based on an asymmetric Salamo-type N₂O₂ ligand. *Z. Anorg. Allg. Chem.* **2015**, *641*, 2520–2524. [[CrossRef](#)]
68. Ma, J.C.; Dong, X.Y.; Dong, W.K.; Zhang, Y.; Zhu, L.C.; Zhang, J.T. An unexpected dinuclear Cu(II) complex with a bis(Salamo) chelating ligand: Synthesis, crystal structure, and photophysical properties. *J. Coord. Chem.* **2016**, *69*, 149–159. [[CrossRef](#)]
69. Li, X.Y.; Kang, Q.P.; Liu, L.Z.; Ma, J.C.; Dong, W.K. Trinuclear Co(II) and mononuclear Ni(II) Salamo-type bisoxime coordination compounds. *Crystals* **2018**, *8*, 43. [[CrossRef](#)]

70. Peng, Y.D.; Li, X.Y.; Kang, Q.P.; An, G.X.; Zhang, Y.; Dong, W.K. Synthesis and fluorescence properties of asymmetrical Salamo-type tetranuclear zinc(II) complex. *Crystals* **2018**, *8*, 107. [[CrossRef](#)]
71. Gao, L.; Liu, C.; Wang, F.; Dong, W.K. Tetra-, penta- and hexa-coordinated transition metal complexes constructed from coumarin-containing N₂O₂ ligand. *Crystals* **2018**, *8*, 77. [[CrossRef](#)]
72. Zheng, S.S.; Dong, W.K.; Zhang, Y.; Chen, L.; Dong, Y.G. Four salamo-type 3d-4f hetero-bimetallic [Zn^{II}Ln^{III}] complexes: Syntheses, crystal structures, and luminescent and magnetic properties. *New J. Chem.* **2017**, *41*, 4966–4973. [[CrossRef](#)]
73. Sun, Y.X.; Zhao, Y.Y.; Li, C.Y.; Yu, B.; Guo, J.Q.; Li, J. Supramolecular cobalt(II) and copper(II) complexes with Schiff base ligand: Syntheses, characterization and crystal structures. *Chin. J. Inorg. Chem.* **2016**, *32*, 913–920.
74. Guo, J.Q.; Sun, Y.X.; Yu, B.; Li, J.; Jia, H.R. Syntheses, crystal structures and spectroscopic properties of copper(II) and nickel(II) complexes with oxime-type Schiff base ligands. *Chin. J. Inorg. Chem.* **2017**, *33*, 1481–1488.
75. Song, X.Q.; Liu, P.P.; Wang, C.Y.; Liu, Y.A.; Liu, W.S.; Zhang, M. Three sandwich-type zinc(II)-lanthanide(III) clusters: Structures, luminescence and magnetic properties. *RSC Adv.* **2017**, *7*, 22692–22698. [[CrossRef](#)]

Sample Availability: Samples of the compounds are available from the authors.



© 2018 by the authors. Licensee MDPI, Basel, Switzerland. This article is an open access article distributed under the terms and conditions of the Creative Commons Attribution (CC BY) license (<http://creativecommons.org/licenses/by/4.0/>).